On the Theory of the Ferrite Resonance Isolator*

E. SCHLÖMANN†

Summary—The attenuation constants for both directions of propagation in a rectangular waveguide loaded with a small slab of ferrite are calculated by means of perturbation theory. The maximum attainable ratio of reverse to forward attenuation is found to be inversely proportional to the square of the bandwidth, with a constant of proportionality that is dependent on the shape of the ferrite slab and the proximity of cutoff. The figure of merit is largest for the case of a thin ferrite slab magnetized perpendicular to the plane of the slab. It is shown that a significant increase in the figure of merit can be obtained by proper use of the anisotropy of grain-oriented materials or single crystals.

I. Introduction

IN this paper the inherent limitations of resonance isolators will be considered. It has been known for some time that the ratio of reverse to forward attenuation cannot exceed a certain optimum value determined by the line width of the ferromagnetic resonance.[1] The bandwidth of resonance isolators has apparently not been considered in any detail up to now. It will be shown that the bandwidth (defined as the frequency range over which the reverse to forward ratio has at least half of its maximum possible value) is proportional to the width of the resonance, with a constant of proportionality that is a rather sensitive function of the shape of the ferrite slab, its magnetization, the frequency, and the cutoff frequency of the waveguide. Under most conditions, the bandwidth is appreciably smaller than the width of the resonance line. It is shown, however, that this situation can be reversed by proper use of magnetocrystalline anisotropy. A device using this effect would require a properly oriented single crystal or grain-oriented polycrystalline material.

We shall consider only the case in which a rectangular waveguide is used. It will be assumed that the cross section of the ferrite slab is very small compared with the cross section of the waveguide, so that a perturbation approach can be used. For simplicity, it is assumed that the unperturbed wave is a TE_{10} mode. It will also be assumed that the ferrite slab or rod has an ellipsoidal cross section. In practice, this configuration is realized by means of circular rods or, approximately, by means of thin slabs of rectangular cross section.

The performance of resonance isolators that use a thin slab of ferrite magnetized in the plane of the slab and perpendicular to the waveguide axis will be investigated in Section II. The geometry of this case is shown in Fig. 1(a). In Section III, the results will be generalized to include the case in which the ferrite slab has an elliptical but otherwise arbitrary cross section, in particular the geometry of Fig. 1(b). The generalization to the case in which a grain-oriented material or a single crystal is used is also given in this section. In Section IV, various assumptions made in the development of the theory will be critically evaluated.

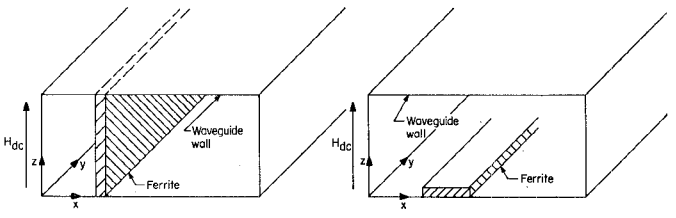

(a) (b)

Fig. 1—(a) Ferrite resonance isolator using a thin ferrite slab magnetized in the plane of the slab. (b) Ferrite resonance isolator using a thin ferrite slab magnetized perpendicular to the plane of the slab. The perturbation theory (1) neglects the variation of the microwave field over the ferrite region, and is valid only if the width of the slab is sufficiently small.

II. Theory

Consider the geometry described in Fig. 1(a). If the cross section of the ferrite slab is much smaller than the cross section of the waveguide, the propagation constant Γ in the presence of the ferrite slab can be calculated by perturbation theory, with the result[1]

$$\Gamma + \Gamma_0^* \sim j\vec{h}^*\overleftrightarrow{\chi}_{\text{eff}}\vec{h}. \tag{1}$$

Here Γ_0 is the propagation constant of the empty waveguide, which is assumed to be lossless (*i.e.*, $\Gamma_0 = j\beta_0$, where β_0 is real). $\overleftrightarrow{\chi}_{\text{eff}}$ is the effective susceptibility, and $\vec{h}$ the RF magnetic field at the site of the ferrite slab. The asterisk denotes the complex conjugate. For a thin slab in the geometry of Fig. 1(a), the effective susceptibility calculated using a Landau-Lifshitz damping term is

$$\overleftrightarrow{\chi}_{\text{eff}} = \frac{M}{(\gamma^2+\lambda^2)H(H+4\pi M) - \omega^2 + 2j\lambda(H+2\pi M)\omega} \cdot \begin{pmatrix} (\gamma^2+\lambda^2)H + j\lambda\omega & j\gamma\omega \\ -j\gamma\omega & (\gamma^2+\lambda^2)(H+4\pi M) + j\lambda\omega \end{pmatrix} \tag{2}$$

where the y-direction is the direction of propagation [see Fig. 1(a)], γ is the gyromagnetic ratio and λ a phenomenological loss parameter which is related to the line width $\Delta H = 2\lambda\omega_0/(\gamma^2+\lambda^2)$. A derivation of (2) is given in Appendix I. The validity of the phenomenological description of losses will be discussed in Section IV.

* Manuscript received by the PGMTT, August 2, 1959; revised manuscript received, November 10, 1959.

† Research Div., Raytheon Co., Waltham, Mass.

[1] B. Lax, "Frequency and loss characteristics of microwave ferrite devices," PROC. IRE vol. 44, pp. 1368–1386; October, 1956.

For a TE_{10} mode, the magnetic field is of the form

$$h_x = j\sqrt{\left(\frac{\omega}{\omega_c}\right)^2 - 1}\sin\phi e^{j\omega t},$$
$$h_y = \cos\phi e^{j\omega t}, \tag{3}$$

where ω_c is the cutoff frequency, ϕ is determined by the position of the slab in the waveguide, and $\phi=0$ and $\phi=\pi$ correspond to the waveguide walls. In (3) the choice of signs is appropriate for a wave propagating in the $+y$-direction, if we let $\phi=0$ characterize the left-hand wall. In order to describe a wave propagating in the $-y$-direction, the sign of the square root has to be reversed. It should be noticed that in the geometry shown and for propagation in the $+y$-direction, the sense of rotation of the transverse magnetic field forms a right-handed screw with the direction of the field. Thus, the $+y$-direction is the reverse direction of the isolator.

From (1), (2), and (3) one obtains the complex propagation constant of the ferrite loaded waveguide. The real part of Γ is the attenuation constant α. Since the empty waveguide was assumed lossless, one finds after trivial calculations for the reverse direction

$$\alpha_{\text{reverse}} \sim \frac{M}{[(\gamma^2+\lambda^2)H(H+4\pi M)-\omega^2]^2+[2\lambda(H+2\pi M)\omega]^2} \cdot \left\{(\gamma^2+\lambda^2)H^2+\omega^2\right]\left[\left(\frac{\omega}{\omega_c}\right)^2-1\right]\sin^2\phi + [(\gamma^2+\lambda^2)(H+4\pi M)^2+\omega^2]\cos^2\phi + 4\gamma(H+2\pi M)\omega\sqrt{\left(\frac{\omega}{\omega_c}\right)^2-1}\sin\phi\cos\phi\right\}. \tag{4}$$

The expression inside the braces can be written as

$$p\sin^2\phi + q\cos^2\phi + 2r\sin\phi\cos\phi = \tfrac{1}{2}[(p+q)-(p-q)\cos 2\phi + 2r\sin 2\phi] \tag{5}$$

where the explicit expressions for p, q, and r are obvious from a comparison with (4). Thus, the condition for maximum (or minimum) reverse attenuation is

$$\tan 2\phi_1 = \frac{-2r}{p-q}. \tag{6}$$

Similarly, the condition for minimum (or maximum) forward attenuation is

$$\tan 2\phi_2 = \frac{2r}{p-q}. \tag{7}$$

Fig. 2 demonstrates the relationship between the two positions ϕ_1 and ϕ_2. It is assumed in this figure that $q>p$. Under these conditions $\phi_1<\phi_2$. It may be seen from Fig. 2 that the position of the ferrite slab, which maximizes the reverse attenuation, coincides with the position, which minimizes the forward attenuation, only

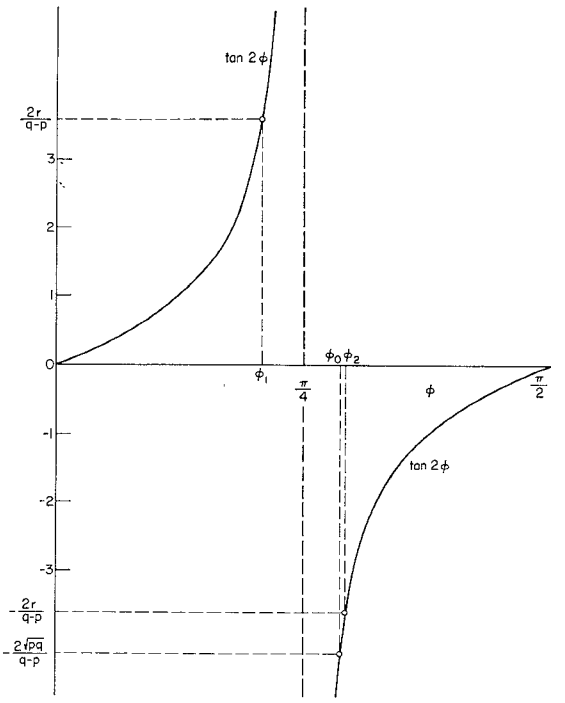

Fig. 2—Graphical determination of the positions of the ferrite slab which maximize the reverse attenuation (ϕ_1), minimize the forward attenuation (ϕ_2), or maximize the reverse to forward ratio (ϕ_0). The full line represents tan 2ϕ.

if $p=q$. Then $\phi_1=\phi_2=\pi/4$; *i.e.*, the distance between ferrite slab and waveguide wall is one quarter of the width of the waveguide. In general, ϕ_1 and ϕ_2 differ from $\pi/4$ in opposite directions by equal amounts.

Similar results have been obtained by Suhl and Walker,[2] who have pointed out that the difference between the energy stored at ϕ in the left-handed wave and in the right-handed wave is proportional to sin 2ϕ. The difference is largest at $\phi=\pi/4$ and $\phi=3\pi/4$, so that large nonreciprocal effects may be expected when the ferrite slab is placed in one of these regions.

The ratio of the two attenuation constants is

$$R(\phi,\omega) = \frac{\alpha_{\text{reverse}}}{\alpha_{\text{forward}}} = \frac{(p+q)-(p-q)\cos 2\phi + 2r\sin 2\phi}{(p+q)-(p-q)\cos 2\phi - 2r\sin 2\phi}. \tag{8}$$

It can be shown that R assumes a maximum with respect to ϕ at ϕ_0 where

$$\cos 2\phi_0 = \frac{p-q}{p+q},$$
$$\sin 2\phi_0 = \frac{2\sqrt{pq}}{p+q}. \tag{9}$$

[2] H. Suhl and L. R. Walker, "Topics in guided wave propagation through gyromagnetic media," *Bell Sys. Tech. J.*, vol. 33, pp. 939–986; July, 1954. See p. 954.

The maximum $R(\omega)$ is thus

$$R_{\max}(\omega) = \frac{\sqrt{pq} + r}{\sqrt{pq} - r} = \frac{\sqrt{[(\gamma^2+\lambda^2)H^2+\omega^2][(\gamma^2+\lambda^2)(H+4\pi M)^2+\omega^2]} + 2\gamma(H+2\pi M)\omega}{\sqrt{[(\gamma^2+\lambda^2)H^2+\omega^2][(\gamma^2+\lambda^2)(H+4\pi M)^2+\omega^2]} - 2\lambda(H+2\pi M)\omega}. \tag{10}$$

Differentiating with respect to ω, one finds that the maximum with respect to ω occurs at $\omega=\omega_0$, where

$$\omega_0^2 = (\gamma^2+\lambda^2)H(H+4\pi M). \tag{11}$$

It can be shown from (7) and (9) that at resonance, ϕ_0 is very close to ϕ_2, the difference being of second order in λ/γ. Fig. 2 illustrates a typical case, where the graphical determination of the various angles for which the two attenuation constants and their ratio are stationary with respect to ϕ.

The maximum reverse to forward ratio is, from (10) and (11),

$$R_{\max}(\omega_0) = \frac{\sqrt{\gamma^2+\lambda^2}+\gamma}{\sqrt{\gamma^2+\lambda^2}-\gamma}. \tag{12}$$

In many cases λ is much smaller than γ. Under these conditions, the exac tformula (12) can be replaced by the first terms of a power series expansion in $(\lambda/\gamma)^2$

$$R_{\max}(\omega) \approx \frac{4\gamma^2}{\lambda^2} + 2 - \frac{1}{4}\frac{\lambda^2}{\gamma^2} + \cdots. \tag{13}$$

Consider the frequency dependence of the reverse to forward ratio in the vicinity of the resonance frequency. Assume that the position of the ferrite slab has been chosen in such a way that the maximum R is achieved. From (8) it is possible to obtain, after trivial calculations (described in Appendix II),

$$R(\phi_0, \omega) = \frac{R_{\max}(\omega_0)}{1+\left[\frac{2(\omega-\omega_0)}{B}\right]^2}. \tag{14}$$

Here $R_{\max}(\omega_0)$ is as given in (12). In the denominator, higher powers of $\omega-\omega_0$ are neglected. According to (14), B is the range of frequencies over which $R(\phi_0, \omega)$ has at least half its maximum value. It will henceforth be called the bandwidth of the isolator. As shown in Appendix II, B to first order in λ/γ is given by

$$B^2 = \frac{2\left(\frac{\lambda}{\gamma}\right)^2\omega_0^2}{1+\frac{1}{a^2}+\frac{1}{2a^4}+\left(1+\frac{1}{a^2}\right)\frac{2\pi M}{\sqrt{(2\pi M)^2+\left(\frac{\omega_0}{\gamma}\right)^2}}} \tag{15}$$

where a is the ratio of the transverse to the longitudinal component of the magnetic field at the resonance frequency (more precisely, the ratio of the transverse field at the center to the longitudinal field at the waveguide wall).

$$a = \sqrt{\left(\frac{\omega_0}{\omega_c}\right)^2 - 1}. \tag{16}$$

A comparison of (13) and (15) shows that a large reverse to forward ratio can usually be obtained only at a sacrifice of bandwidth, and vice versa. Therefore, it is reasonable to take this fact into account in the definition of the figure of merit of the isolator. In the existing literature, the reverse to forward ratio itself has sometimes been called the figure of merit. This is a reasonable choice only if the bandwidth of the device is immaterial. We shall adopt a different convention and define the figure of merit as

$$F = R_{\max}\left(\frac{B}{\omega_0}\right)^2. \tag{17}$$

A comparison of (13), (15), and (17) shows that with this definition, the figure of merit is approximately independent of the loss parameter λ. If higher powers of λ/γ are neglected, one obtains

$$F = \frac{8}{1+\frac{1}{a^2}+\frac{1}{2a^4}+\left(1+\frac{1}{a^2}\right)\frac{2\pi M}{\sqrt{(2\pi M)^2+\left(\frac{\omega}{\gamma}\right)^2}}}. \tag{18}$$

Since all terms in the denominator of (18) are positive, the larger a and ω are, and the smaller M is, the greater the figure of merit becomes. If $2\pi M \ll \omega/\gamma$, the last term in the denominator is only a small correction. As a particular example, consider the case where the frequency is 2800 mc and $2\pi M$ is 1000 gauss. For practical purposes, a^2 cannot be made larger than 3. For this particular value, the frequency equals twice the cutoff frequency for TE_{10} modes and is thus equal to the cutoff frequency for TE_{20} modes. The figure of merit for $a^2=3$ and for the given values of magnetization and frequency is approximately 3.5.

III. Generalizations

The theory presented in the previous section can easily be generalized in such a way that it will apply to situations in which the ferrite slab has an elliptical but otherwise arbitrary cross section and the dc field is applied along an axis of the ellipse. In the latter situation, the transverse demagnetizing field is $4\pi MN$ rather than $4\pi M$ as previously. Here N is the transverse demagnet-

izing factor.[3] Similarly, H must now be interpreted as the internal or "demagnetized" field

$$H = H_{\text{app}} - 4\pi M N_z. \tag{19}$$

Here N_z is the longitudinal demagnetizing factor. All significant results derived previously can be taken over immediately if $4\pi M$ is replaced by $4\pi MN$. There are minor exceptions to this rule, namely, the factors M that occur (2), (4), (30), and (31).[4] It is easily seen, however, that these factors cancel out in all the significant results, such as the positions for minimum or maximum attenuations, maximum reverse to forward ratio, bandwidth, and figure of merit. In particular, one obtains for the figure of merit

$$F = \frac{8}{1+\frac{1}{a^2}+\frac{1}{2a^4}+\left(1+\frac{1}{a^2}\right)\frac{2\pi MN}{\sqrt{(2\pi MN)^2+\left(\frac{\omega_0}{\gamma}\right)^2}}}. \tag{20}$$

Thus, for given a, M, and ω, the best figure of merit is obtained when N is very small. This can be realized in the situation described in Fig. 1(b), in which a thin slab is placed on the bottom of the waveguide and magnetized in a direction which is perpendicular to the plane of the slab. Under these conditions, the figure of merit for $a^2=3$ is approximately 5.75; *i.e.*, 65 per cent larger than the figure of merit calculated previously for the geometry of Fig. 1(a).

M. T. Weiss[5] has reported measurements of the performance characteristics of resonance isolators using rectangular waveguides and ferrite configurations which are similar to those of Fig. 1. For the configuration of Fig. 1(b) ("H-plane isolator"), he obtained the following results: $R_{\max}=75$, $B/\omega_0=0.16$. The figure of merit as experimentally determined is thus, according to (17), $F_{\text{exp}}\approx 2$. The theoretical formula (20), on the other hand, leads to $F_{\text{theor}}\approx 3.2$. In this calculation we have used a transverse demagnetizing factor appropriate for a rod of ellipsoidal cross section with an axial ratio equal to that of the rectangular slab used in the device. The parameter a of (20) was deduced from the width of the waveguide (0.9 inch) with the help of (16). Weiss has also reported measurements on "E-plane isolators" using configurations similar to Fig. 1(a). In these cases, however, a dielectric slab with a high dielectric constant was placed adjacent to the ferrite slab. The figures of merit as deduced from his data for two such configurations are 0.9 and 0.5, respectively. The theoretical formula (20), on the other hand, predicts figures of merit of approximately 2.7 and 2.2 in the two cases. It should be remembered, however, that this formula does not take into account the effect of the dielectric slab. For this reason, the lack of agreement between theory and experiment in the E-plane geometry is not too serious. It thus appears that (20) is at least qualitatively applicable for typical device configurations even though it was derived on the basis of perturbation theory.

In the H-plane geometry of Fig. 1(b), the free precession of the magnetization vector follows a circular cone. In the E-plane geometry of Fig. 1(a), however, the circle is distorted by the transverse demagnetizing field into an ellipse which has its major axis lying in the plane of the slab; *i.e.*, in the direction of propagation. Since the figure of merit is larger in the H-plane geometry than in the E-plane geometry, one may surmise that a further increase in the figure of merit can be obtained by forcing the free precession to follow an ellipsoidal cone with the major axis of the ellipse oriented so that it is perpendicular to the direction of propagation. The calculation presented below shows that this is the case. The ferrite slab must consist of a single crystal or of grain-oriented polycrystalline material. In the presence of crystalline anisotropy, the precessing magnetization generally follows an ellipsoidal cone, unless the dc field is applied along an axis of high symmetry (like the [100] or [111] axes of cubic crystals). The orientation of the single crystal obviously has to be such that through anisotropy forces the magnetization vector is repelled more strongly from the y-direction than from the x-direction. If the material has hexagonal crystal structure, the desired effect can be obtained if the first-order anisotropy constant is negative (*i.e.*, if the plane perpendicular to the hexagonal axis is energetically preferred over the axis). In this case, the orientation should be such that the hexagonal axis coincides with the waveguide axis (y-direction). The desired effect can also be obtained with cubic materials. In this case, the orientation should be such that the field direction (z-direction) coincides with a [110] direction. If the first-order cubic anisotropy constant is positive, a [100] direction should be aligned with the waveguide axis; if it is negative, a [110] direction should be aligned with this axis.

We shall consider in detail only the case of a hexagonal material with a preferential plane. The generalization to the cubic case is, however, very straightforward. In the hexagonal case, the anisotropy repels the magnetization only from the y-direction and has no effect in the x-direction. The additional energy (per unit volume) in this case is

$$E_{\text{anis}} = \frac{M}{2} H_a \alpha_y^2 \tag{21}$$

where $H_a = 2|K_1|/M$ is the anisotropy field and α_y the directional cosine of the magnetization with the y-direction. This energy has to be added to the energy given in (30). It is obvious that the energy appropriate for a

[3] In the present notation, the sum of the three principal demagnetizing factors equals unity.

[4] The notation in the present paper is such that M has the factor π in all those cases in which it should be changed to MN. It does not have this factor in all other cases.

[5] M. T. Weiss, "Improved rectangular waveguide resonance isolators," IRE TRANS. ON MICROWAVE THEORY AND TECHNIQUES, vol. MTT-4, pp. 240–243; October, 1956.

situation in which the ferrite slab has a transverse demagnetizing factor N and the anisotropy is of the form described above, is of essentially the same form as that given in (30). It can be formally obtained from (30) if H is replaced by $H+H_a$ and $4\pi M$ is replaced by $4\pi MN-H_a$. Thus, all the significant results obtained previously can be generalized by applylng the same rule. In particular, the figure of merit now becomes

$$F = \frac{8}{1+\frac{1}{a^2}+\frac{1}{2a^4}-\left(1+\frac{1}{a^2}\right)\frac{H_a-4\pi MN}{\sqrt{(H_a-4\pi MN)^2+\left(2\frac{\omega_0}{\gamma}\right)^2}}}. \tag{22}$$

A comparison of (20) and (22) shows immediately that a significant increase in the figure of merit can be obtained if $(H_a-4\pi MN)$ is much larger than $2\omega_0/\gamma$. The ultimate figure of merit according to (22) is

$$F_{\max} = 16a^4.$$

Thus, for $a^2=3$, $F_{\max}=144$; *i.e.*, a factor of 25 better than the previous optimum value. In practice, it will be very difficult to obtain this ultimate figure of merit because the internal magnetic field necessary to produce resonance decreases to zero as the optimum condition is approached. Thus it is eventually not strong enough to magnetize the material. A numerical example that can probably be realized is the following: $4\pi M=2000$ gauss, $N=1/20$, $H_a=2000$ oersteds, $f=2800$ mc, $a^2=3$. The internal magnetic field at resonance is 330 oersteds, and the figure of merit is 17. If $H_a=3000$ oersteds and everything else is unchanged, the internal field at resonance is 210 oersteds, and the figure of merit is 27.5.

IV. Discussion

The theory presented in the preceding sections makes extensive use of a phenomenological description of damping forces. This phenomenological approach cannot be justified on a rigorous basis. It can be shown, however, that a microscopic theory of some of the important loss mechanisms leads to essentially equivalent results. A slight generalization is necessary: the loss parameter λ is, in general, a function of frequency and internal magnetic field.

For a discussion of the resonance isolator, it is important to consider the absorption of radiation which has the negative sense of circular polarization. This absorption, although small, limits the reverse to forward ratio of a resonance isolator. In a previous publication,[6] the present author has developed a theory of line broadening in polycrystalline ferrites, and has briefly discussed the absorption of radiation with the negative sense of circular polarization. According to this theory, the susceptibility for circular polarization is essentially given by[7]

$$\chi_+(\omega) = \frac{\gamma M}{\omega_0-\omega+j(W_p-W_q)}. \tag{23}$$

Here W_p and W_q are functions of frequency and magnetic field which are discussed in an earlier paper.[6] It can be shown that W_p and W_q are non-negative, that W_p is nonzero only for $\omega>0$ (positive sense of circular polarization), and that W_q is nonzero only for $\omega<0$ (negative sense of circular polarization). For the particular mechanism investigated in the earlier paper,[6] it can also be shown that $W_p(\omega)$ is approximately equal to $W_q(-\omega)$. The circular susceptibility for the negative sense of polarization is obtained from (23) by inverting the sign of ω and taking the complex conjugate.

On the other hand, the circular susceptibility as calculated from the phenomenological equations is

$$\chi_+(\omega) = \frac{M}{H-\frac{\omega}{\gamma+j\lambda}} = \frac{\frac{\gamma^2+\lambda^2}{\gamma}M}{\frac{\gamma^2+\lambda^2}{\gamma}H-\omega+j\omega\frac{\lambda}{\gamma}}. \tag{24}$$

A comparison of (23) and (24) shows immediately that the two results are nearly equivalent if $\lambda/\gamma\ll 1$ and if we allow λ to be dependent on frequency and magnetic field. In this sense, the phenomenological description used in this paper is justified.

It is interesting to compare the bandwidth of the isolator (as defined in Section II) with the width of the ferromagnetic resonance (*i.e.*, the frequency range over which the reverse attenuation has at least half of its maximum value). The width of the resonance can easily be obtained from (4). The numerator of the right-hand side of this equation is relatively insensitive to small changes in frequency around the resonance frequency. The denominator, however, is very sensitive. One finds that to first order in λ/γ, the half width of the resonance for the geometry of Fig. 1(a) is

$$\Delta\omega = 2\lambda(H+2\pi M) = 2\lambda\sqrt{\left(\frac{\omega_0}{\gamma}\right)+(2\pi M)^2}. \tag{25}$$

An expression appropriate for other geometries is obtained by replacing M by MN. It should be remem-

[6] E. Schlömann, "Spin-wave analysis of ferromagnetic resonance in polycrystalline ferrites," *J. Phys. Chem. Solids*, vol. 6, no 213, pp. 242–256; 1958.

[7] *Ibid.*, (42) and (43). The equation given in the present paper is simplified by the assumption of vanishing "intrinsic" loss and neglect of the shift of the resonance frequency.

bered, however, that the phenomenological constant λ is also dependent on the demagnetizing factor. The reason for this is as follows: λ depends primarily on the frequency and the internal (demagnetized) magnetic field. A change in the demagnetizing factor at fixed frequency produces a change in the internal field at resonance. In this way, λ is implicitly dependent on N. The theory described in the earlier work[6] predicts that λ should be largest for the geometry of Fig. 1(a), smallest for the geometry of Fig. 1(b). A comparison of (25) with (15) shows that for nonoriented polycrystalline material, the bandwidth is at least a factor $\sqrt{2}$ smaller than the width of the resonance.

Consider finally the half width of the resonance determined by varying the magnetic field at constant frequency. From (4) one finds for the geometry of Fig. 1(a) to first order in λ/γ

$$\Delta H = 2\frac{\lambda\omega_0}{\gamma^2}. \tag{26}$$

The same expression is valid for an arbitrary demagnetizing factor. It is thus also valid for the geometry of Fig. 1(b). Eq. (26) shows that the phenomenological parameter λ appropriate for a given geometry can be obtained experimentally by observing the line width ΔH. The maximum reverse to forward ratio is therefore, from (13) and (26), approximately

$$R_{\max} \approx 16\left(\frac{\omega_0}{\gamma\Delta H}\right)^2. \tag{27}$$

Here ΔH should be measured at the same frequency and with the same geometry that is actually used in the isolator.

The most significant results of the present investigation are the observation that the bandwidth is usually appreciably smaller than the width of the resonance line, and the prediction that the figure of merit can be appreciably increased by proper use of grain-oriented materials. Since these results are not at all obvious, it is worthwhile to try to understand in a simple way the reasons for this behavior.

In this connection, it is important to realize that the forward attenuation plays a decisive part in determining the reverse to forward ratio. It is easily seen that at resonance the condition for minimum forward attenuation (7) coincides to first order in λ/γ with the condition for maximum reverse to forward ratio (9). It is very possible, therefore, that the bandwidth of the isolator is not the same as the width of the resonance. The phenomenon which primarily determines the bandwidth is the frequency dependence of the ratio of the transverse to the longitudinal components of the magnetic field, because this effect gives rise to a rather strong frequency dependence of the forward attenuation. For this reason the bandwidth is dependent, among other things, on the ratio of the resonance frequency and the cutoff frequency, and vanishes as this ratio approaches unity.

To obtain a better intuitive understanding of the situation, it is advantageous to consider the frequency dependence of ϕ_0, *i.e.*, the position of the ferrite slab that results in a maximum reverse to forward ratio. For the geometry of Fig. 1(a), one finds from (9) and the remarks at the beginning of Appendix II that ϕ_0 is determined by

$$\tan^2\phi_0 = \frac{q}{p} = \frac{(\gamma^2+\lambda^2)(H+4\pi M)^2 - \omega^2}{[(\gamma^2+\lambda^2)H^2-\omega^2]\left[\left(\frac{\omega}{\omega_c}\right)^2 - 1\right]}. \tag{28}$$

By straightforward differentiation, one obtains the fractional change of $\tan\phi_0$, divided by the fractional change of the frequency taken at resonance.

$$\frac{\omega_0}{\tan\phi_0}\left.\frac{d\tan\phi_0}{d\omega}\right|_{\omega=\omega_0} = -\left\{1+\frac{1}{a^2}+\frac{2\pi M}{\sqrt{(2\pi M)^2+\frac{\omega_0^2}{\gamma^2+\lambda^2}}}\right\}. \tag{29}$$

This equation can again be generalized to the case of a ferrite slab with an arbitrary transverse demagnetizing factor N and an anisotropy field H_a by replacing $4\pi M$ by $4\pi MN - H_a$. Eq. (29) shows that the frequency dependence of ϕ_0 is weakest for large a and small N. By proper use of grain-oriented materials, the sign of the last term of (29) can effectively be reversed. In the limit as $H_a \gg 2\omega_0/\gamma$ this term approaches -1. It is thus seen that the frequency dependence of ϕ_0 can be significantly reduced by the use of grain-oriented materials. It is easy to believe, therefore, that the figure of merit of the isolator should be improved in a similar way.

Appendix I

Effective Susceptibility of a Thin Slab

The equation of motion can be derived conveniently from the energy (per unit volume) necessary to pull the magnetization vector out of the z-direction into a direction characterized by the two directional cosines, α_x and α_y. This energy is for a thin slab in the geometry of Fig. 1(a) and for $\alpha_x, \alpha_y \ll 1$.

$$E = \frac{M}{2}\{(H+4\pi M)\alpha_x^2 + H\alpha_y^2\} - M(\alpha_x h_x + \alpha_y h_y). \tag{30}$$

The equations of motion are now

$$\begin{aligned} M\dot{\alpha}_x &= -\gamma\frac{\partial E}{\partial \alpha_y} - \lambda\frac{\partial E}{\partial \alpha_x} \\ M\dot{\alpha}_y &= \gamma\frac{\partial E}{\partial \alpha_x} - \lambda\frac{\partial E}{\partial \alpha_y}. \end{aligned} \tag{31}$$

If the driving field has a periodic time dependence ($\sim e^{j\omega t}$), one obtains from (30) and (31)

$$\begin{aligned} [j\omega + \lambda(H+4\pi M)]\alpha_x + \gamma H\alpha_y &= \gamma h_y + \lambda h_x \\ \gamma(H+4\pi M)\alpha_x - [j\omega + \lambda H]\alpha_y &= \gamma h_x - \lambda h_y. \end{aligned} \tag{32}$$

By solving (32) for α_x and α_y, it is easy to obtain the effective susceptibillty given in (2). The same result can also be derived by converting the "true" susceptibility $\overleftrightarrow{\chi}$ (as calculated using a Landau-Lifshitz damping term) to the effective susceptibility by using the formula

$$\overleftrightarrow{\chi}_{\text{eff}} = (1 + 4\pi\overleftrightarrow{\chi}\overleftrightarrow{N})^{-1}\overleftrightarrow{\chi}. \tag{33}$$

Appendix II

Isolator Bandwidth

In evaluating the bandwidth, it is convenient to use the left-hand side of (5), thus expressing R in terms of $\cos\phi$ and $\sin\phi$ rather than $\cos 2\phi$ and $\sin 2\phi$. Since (9) is equivalent to

$$\cos\phi_0 = \sqrt{\frac{p}{p+q}} \quad \sin\phi_0 = \sqrt{\frac{q}{p+q}} \tag{34}$$

one obtains from (5) and (8)

$$R(\phi_0, \omega) = \frac{N(\omega)}{D(\omega)} \tag{35}$$

where

$$\begin{aligned} N(\omega) = {} & [(\gamma^2+\lambda^2)H^2 + \omega^2][(\gamma^2+\lambda^2)(H+4\pi M)^2 + \omega_0^2] \\ & \cdot\left[\left(\frac{\omega}{\omega_c}\right)^2 - 1\right] \\ & + [(\gamma^2+\lambda^2)H^2 + \omega_0^2][(\gamma^2+\lambda^2)(H+4\pi M)^2 + \omega^2] \\ & \cdot\left[\left(\frac{\omega_0}{\omega_c}\right)^2 - 1\right] \\ & + 4\gamma(H+2\pi M)\omega \\ & \cdot\left\{[(\gamma^2+\lambda^2)H^2 + \omega_0^2][(\gamma^2+\lambda^2)(H+4\pi M)^2 + \omega_0^2]\right. \\ & \left.\cdot\left[\left(\frac{\omega_0}{\omega_c}\right)^2 - 1\right]\left[\left(\frac{\omega}{\omega_c}\right)^2 - 1\right]\right\}^{1/2} \end{aligned} \tag{36}$$

and $D(\omega)$ is obtained from $N(\omega)$ by reversing the sign of γ.

Now let $\omega = \omega_0 + \delta\omega$. Neglecting higher powers of $\delta\omega$, one finds

$$\left[\left(\frac{\omega}{\omega_c}\right)^2 - 1\right]^{1/2} = a\left\{1 + \frac{\omega_0\delta\omega}{a^2\omega_c^2} - \frac{(\delta\omega)^2}{2a^4\omega_c^2}\right\} \tag{37}$$

where

$$a = \sqrt{\left(\frac{\omega_0}{\omega_c}\right)^2 - 1}$$

is the ratio of the amplitudes of the transverse and longitudinal components of the magnetic field. Expanding $N(\omega)$ in powers of $\delta\omega$, one obtains

$$N(\omega) = N_0 + N_1\delta\omega + N_2(\delta\omega)^2 + \cdots \tag{38}$$

where

$$N_0 = 8(\gamma^2+\lambda^2)(H+2\pi M)^2\omega_0^2a^2\left(1 + \frac{\gamma}{\sqrt{\gamma^2+\lambda^2}}\right)$$

$$N_1 = 8(\gamma^2+\lambda^2)(H+2\pi M)^2\omega_0(2a^2+1) \cdot\left(1 + \frac{\gamma}{\sqrt{\gamma^2+\lambda^2}}\right)$$

$$\begin{aligned} N_2 = {} & 4(\gamma^2+\lambda^2)(H+2\pi M) \\ & \cdot\left\{(4H+12\pi M)a^2 + (3H+10\pi M)\right. \\ & \left. + \frac{\gamma}{\sqrt{\gamma^2+\lambda^2}}(H+2\pi M)\left(2a^2+1-\frac{1}{a^2}\right)\right\}. \end{aligned} \tag{39}$$

From (35), (38), and (39) the reverse to forward ratio is

$$R(\phi_0, \omega) = R_{\max}(\omega_0)\,\frac{1 + \alpha_1\delta\omega + \alpha_2(\delta\omega)^2}{1 + \beta_1\delta\omega + \beta_2(\delta\omega)^2} \tag{40}$$

where

$$\alpha_1 = \beta_1 = \frac{N_1}{N_0} = \frac{2a^2+1}{\omega_0 a^2}$$

$$\alpha_2 = \frac{(4H+12\pi M)a^2 + (3H+10\pi M) + \dfrac{\gamma}{\sqrt{\gamma^2+\lambda^2}}(H+2\pi M)\left(2a^2+1-\dfrac{1}{a^2}\right)}{2(H+2\pi M)\omega_0^2a^2\left(1+\dfrac{\gamma}{\sqrt{\gamma^2+\lambda^2}}\right)} \tag{41}$$

and β_2 is obtained from α_2 by reversing the sign of γ. It is obvious from (41) that β_2 is much larger than α_2 for $\lambda/\gamma \ll 1$. For this reason an expansion of R in powers of $\delta\omega$ converges very slowly, but an expansion of $1/R$ in powers of $\delta\omega$ should converge rapidly. If higher powers of $\delta\omega$ are again neglected, (14) is obtained from (40) and

$$\left(\frac{2}{B}\right)^2 = \beta_2 - \alpha_2. \tag{42}$$

A simple expression for the bandwidth is obtained in the limit $\lambda/\gamma \ll 1$. The α_2 term of (42) can be neglected if only the lowest order of λ/γ is taken into account. In this approximation

$$B^2 = \frac{4}{\beta_2} = \frac{2(\lambda/\gamma)^2\omega_0^2}{1 + \frac{1}{a^2} + \frac{1}{2a^4} + \left(1 + \frac{1}{a^2}\right)\frac{2\pi M}{H + 2\pi M}}. \tag{43}$$

Eq. (15) is now obtained by expressing H in terms of the resonance frequency.

Analysis of Microwave Measurement Techniques by Means of Signal Flow Graphs*

J. K. HUNTON†

Summary—**Microwave measurement techniques can be analyzed more simply by using signal flow graphs instead of the customary scattering matrices to describe the microwave networks used in the measuring system. This is because the flow graphs of individual networks are simply joined together when the networks are cascaded and the solution for the system can be written down by inspection of the over-all flow graph by application of the nontouching loop rule. This paper reviews the method of setting up flow graphs of microwave networks and the rule for their solution. A single directional-coupler reflectometer system for measuring the reflection coefficient of a load is then analyzed by this method. The analysis shows how auxiliary tuners can be used to cancel residual error terms in the measurement of the magnitude of the reflection coefficient at a particular frequency. The analysis also shows how an additional tuner can be used to measure the phase angle of the reflection coefficient. These reflectometer techniques are particularly useful in the measurement of very small reflections.**

Introduction

THE signal flow graph is a method of writing a set of equations, whereby the variables are represented by points and the interrelations by directed lines giving a direct picture of signal flow. The algebra of flow graphs leading to solutions by direct inspection has been developed by S. J. Mason and others at the Massachusetts Institute of Technology.[1,2] When microwave network equations are written in scattering matrix form the corresponding flow graph is particularly useful because, in this case, the flow graph of a system of cascaded networks is constructed simply by joining together the flow graphs of the individual networks, and the solution is then available directly.

One of the best applications of the flow graph method is in the analysis of measuring techniques and the determination of residual errors. It is the intention here to review the mechanics of the method and to apply it in analyzing the microwave reflectometer system used for measuring the reflection coefficient of a load. This system has been in general use for some time,[3] and has been analyzed recently by Engen and Beatty[4] who showed how tuners could be used to reduce residual errors to a negligible value when measuring the magnitude of the reflection coefficient. Their result will be derived here by the flow graph method. In addition, a technique for measuring the phase angle of the reflection coefficient will be presented.

One- and Two-Port Network Flow Graphs

Fig. 1 shows some simple flow graphs used as building blocks. In Fig. 1(a) the general two-port network is shown as specified by its scattering matrix coefficients. Here a_1 and a_2 are the complex entering wave amplitudes, while b_1 and b_2 are the outgoing wave amplitudes at ports 1 and 2 of the network. These are represented in the flow graph as points or "nodes." The nodes are

* Manuscript received by the PGMT, September 14, 1959; revised manuscript received November 25, 1959.

† Hewlett-Packard Co., Palo Alto, Calif.

[1] S. J. Mason, "Feedback theory—some properties of signal flow graphs," PROC. IRE, vol. 41, p. 1144–1156; September 1953.

[2] S. J. Mason, "Feedback theory—further properties of signal flow graphs," PROC. IRE, vol. 44, pp. 920–926; July, 1956.

[3] J. K. Hunton and N. L. Pappas, "The -hp- microwave reflectometers," *Hewlett-Packard J.*, vol. 6, pp. 1–7; September–October; 1954.

[4] G. F. Engen and R. W. Beatty, "Microwave reflectometer techniques," IRE TRANS. ON MICROWAVE THEORY AND TECHNIQUES, vol. MTT-7, pp. 351–355; July 1959.